atoms

MDPI

Article

Photoejection from Various Systems and Radiative-Rate Coefficients

Anand K. Bhatia

Heliophysics Science Division, NASA/Goddard Space Flight Center, Greenbelt, MD 20771, USA; anand.k.bhatia@nasa.gov

Abstract: Photoionization or photodetachment is an important process. It has applications in solar- and astrophysics. In addition to accurate wave function of the target, accurate continuum functions are required. There are various approaches, like exchange approximation, method of polarized orbitals, close-coupling approximation, R-matrix formulation, exterior complex scaling, the recent hybrid theory, etc., to calculate scattering functions. We describe some of them used in calculations of photodetachment or photoabsorption cross sections of ions and atoms. Comparisons of cross sections obtained using different approaches for the ejected electron are given. Furthermore, recombination rate coefficients are also important in solar- and astrophysics and they have been calculated at various electron temperatures using the Maxwell velocity distribution function. Approaches based on the method of polarized orbitals do not provide any resonance structure of photoabsorption cross sections, in spite of the fact that accurate results have been obtained away from the resonance region and in the resonance region by calculating continuum functions to calculate resonance widths using phase shifts in the Breit–Wigner formula for calculating resonance parameters. Accurate resonance parameters in the elastic cross sections have been obtained using the hybrid theory and they compare well with those obtained using the Feshbach formulation. We conclude that accurate results for photoabsorption cross sections can be obtained using the hybrid theory.

Keywords: scattering functions; photoabsorption; photoionization; radiative attachment; opacity

Citation: Bhatia, A.K. Photoejection from Various Systems and Radiative-Rate Coefficients. *Atoms* **2022**, *10*, 9. https://doi.org/10.3390/atoms10010009

Academic Editors: Sultana N. Nahar and Guillermo Hinojosa

Received: 17 November 2021
Accepted: 14 January 2022
Published: 19 January 2022

1. Introduction, Calculations and Results

In 1865, J. C. Maxwell proposed his theory of propagation of electromagnet waves. In 1887, experiments of H. Hertz confirmed his theory. His experiments also showed the existence of discrete energy levels and led to Einstein's photoelectric law [1]. In a photoelectric effect, photons behave like particles rather than waves, as also in the experiment on the scattering of X-rays by electrons by A. H. Compton [2]. This was also confirmed by the experiments of Bothe and Geiger [3]. Their experiments showed that the electron moved from its position in about 10^{-7} s. A wave would have taken much longer to move the electron. Photodetachment of negative hydrogen ions is given by

$$h\nu + H^- \rightarrow e + H \tag{1}$$

It was suggested by Wildt [4] that this process is an important source of opacity in the atmosphere of the Sun, in addition to processes like bound-bound transitions, free-free transitions, and Thomson scattering. The cross section, in units of Bohr radius, for this process in the length form and in the dipole approximation is given by (cf. Appendix A)

$$\sigma(a_0^2) = 4\alpha\pi k(I + k^2)\left|\left\langle \Psi_f \middle| z_1 + z_2 \middle| \Phi \right\rangle\right|^2 \tag{2}$$

In the above expression, $\alpha = 1/137.036$ is the fine structure constant, I is the ionization potential, $z_i = r_i \cos(\theta_i)$ are the dipole transition operators, and k is the momentum of the outgoing electron. Rydberg units are used in this article. The function Φ represents the

bound state wave function of the hydrogen ion and Ψ_f is the wave function of the outgoing electron and the remaining hydrogen atom. Various approximations have been made for the scattering function.

The simplest approximation is the exchange approximation given by

$$\Psi(\vec{r}_1, \vec{r}_2) = u(\vec{r}_1)\phi(\vec{r}_2) \pm (1 \leftrightarrow 2) \tag{3}$$

In the above equation, $\vec{r}_1$ and $\vec{r}_2$ are the distances of the incident and bound electrons from the nucleus, assumed fixed, so that the recoil of the nucleus can be neglected, $u(\vec{r}_1)$ is the scattering function and $\phi(\vec{r}_2)$ is the target function. Exchange between similar particles is important. The plus sign refers to the singlet states and the minus sign refers to triplet states. In these equations

$$u(\vec{r}_1) = \frac{u(r_1)}{r_1} Y_{Lo}(\theta_1, \phi_1) \tag{4}$$

The angles θ_1 and φ_1 are the spherical polar angles, measured in radians. The ground state function is given by

$$\phi(\vec{r}_2) = 2e^{-r_2} Y_{00}(\theta_2, \phi_2) \tag{5}$$

The scattering function u of the incident particle is obtained from

$$\int Y_{lo}(\Omega_1)\phi_0(\vec{r}_2)\Big|H - E\Big|\Psi(\vec{r}_1, \vec{r}_2)d\Omega_1 d\vec{r}_2 = 0 \tag{6}$$

Morse and Allis [5] carried out the exchange approximation calculations in 1933. Assuming that the nucleus is of infinite mass, is fixed, and the recoil of the nucleus can be neglected, the Hamiltonian H and energy E (in Rydberg units) are given by

$$H = -\nabla_1^2 - \nabla_2^2 - \frac{2Z}{r_1} - \frac{2Z}{r_2} + \frac{2}{r_{12}} \tag{7}$$

$$E = -Z^2 + k^2 \tag{8}$$

Z is the nuclear change and k is the momentum of the incident particle. Using Equation (6), we get the equation for the scattering function

$$[\frac{d^2}{dr^2} - \frac{l(l+1)}{r^2} + v_d r_1 + k^2]u_l(r_1) \pm 4Z^2[(Z^2 + k^2)\delta_{l0} r_1 V_l(r_1) - \frac{2}{2l+1} y_l(r_1)] = 0 \tag{9}$$

$$v_d(r) = \frac{2(Z-1)}{r} + 2e^{-Zr}(1 + \frac{1}{r}) \tag{10}$$

$$y_l(r) = \frac{1}{r^l}\int_0^r x^{l+1}\phi_0(x)u_l(x)dx + r^{l+1}\int_r^\infty \phi_0(x)\frac{u_l(x)}{x^l}dx \tag{11}$$

$$V_l = \int_0^\infty e^{-Zx} x u_l(x) dx \tag{12}$$

In Equation (9), δ_{lo} is the Dirac delta function. The scattering function behaves asymptotically like $\sin(kr - l\frac{\pi}{2} + \eta_l)$, where η_l is the phase shift for the incident electron of angular momentum l.

The target electron is distorted because of the electric field produced by the incident electron, resulting in a lowering of the energy by $\Delta E = -\frac{1}{2}\alpha E_e^2$, where $\alpha = 4.5a_0^3$ is the polarizability of the hydrogen atom and E_e is the electric field produced by the incident electron. For a slowly moving incident electron, this distortion has been taken into account by the method of polarized orbitals of Temkin [6], assuming that the atom follows the

instantaneous motion of the scattered electron. He proved that the target function, now polarized, for an incident electron at a distance r_1 is given by

$$\Phi^{pol}(\vec{r}_1, \vec{r}_2) = \phi_0(\vec{r}_2) - \frac{\varepsilon(r_1, r_2)}{r_1^2} u_{1s\to p}(\vec{r}_2) \tag{13}$$

$$u_{1s\to p}(\vec{r}_2) = \frac{\cos\theta_{12}}{(Z\pi)^{0.5}} e^{-Zr_2}\left(\frac{Z}{2}r_2^2 + r_2\right) \tag{14}$$

In Equation (13), $\varepsilon(r_1, r_2)$ is a step function which allows polarization of the target electron only when the incident electron is outside the orbit of the target because the step function is equal to 1 when r_1 is greater than r_2, zero otherwise. The integro-differential equation for the function $u(r_1)$ for all angular momenta has been given by Sloan [7]. The method of polarized orbitals has been used extensively for atoms as well as for molecules. However, this method is not variationally correct, and only the long-range correlations can be included.

The method has been modified in the hybrid theory [8] by replacing the step function $\varepsilon(r_1, r_2)$ by a cutoff function $\chi(r_1) = (1 - e^{-\beta r_1})^n$, where β and n are optimized to get the maximum phase shifts and now the polarization of the target takes place whether the incident electron is inside or outside the orbit of the target electron. Phase shifts have lower bounds, i.e., they are always below the exact phase shifts, but approaching the correct value as the number of short-range correlations is increased. Short-range correlations are also included by writing the wave function as

$$\Psi(\vec{r}_1, \vec{r}_2) = u(\vec{r}_1)\Phi^{pol}(\vec{r}_1, \vec{r}_2) + (1 \leftrightarrow 2) + \sum C_i \Phi_l^i(\vec{r}_1, \vec{r}_2) \tag{15}$$

The last term in the above equation representing correlation functions for any angular momentum l are of the Hylleraas type. The equation for the scattering function is now obtained from

$$\int d\Omega_1 d\vec{r}_2 Y_{lo}(\Omega_1)\Phi^{pol}\Big|H - E\Big|\Psi(\vec{r}_1, \vec{r}_2) = 0 \tag{16}$$

In the above equation, H is the Hamiltonian of the system and E is the energy.

The resulting equation is given in Ref. [8]. This formulation gives accurate phase shifts and resonance parameters of He atoms and Li^+ ions. The results compare well with those obtained using other approaches.

The initial state Φ in Equation (2) can be a (1s1s) ^1S state or (1s2s) $^{1,3}S$ states. This function Φ can be chosen of the Hylleraas form and is accurately known when calculating energy of the state by the Rayleigh–Ritz variational principle and the final state function can be calculated accurately using the hybrid theory or any other approach. Cross sections have been calculated using the Hylleraas functions with 364 terms for the initial state function, and when 35 short-range correlations are also included in the final state wave function, as indicated in Equation (15). These results are given in Table 1 of ref. [9] and are now given here in Table 1. We see that the inclusion of the short-range correlations does change the cross sections slightly. Bell and Kingston [10], using the method of polarized orbitals, also calculated these cross sections. Their results are also given in Table 1 along with the close-coupling results of Wishart [11], who used the close-coupling approximation for the continuum functions. We find that the results of ref. [10] differ from those calculated using the hybrid theory which provides accurate scattering functions.

Table 1. Photodetachment cross section (Mb) of H^-.

k	Cross Section without Short-Range Correlations	Cross Sections with Short-Range Correlations	Bell and Kingston, Ref. [10]	Wishart, Ref. [11]
0.01	0.0245	-	-	-
0.02	0.1959	-	-	-
0.03	0.6444	-	-	-
0.04	1.4736	1.4750	-	-
0.05	2.7480	2.7517	-	-
0.06	4.4914	4.4988	-	-
0.07	6.6844	-	-	-
0.1	15.2465	15.3024	12.34	15.937
0.2	38.3688	38.5443	40.48	37.870
0.23	39.4354	39.6366	-	38.707
0.24	39.2882	-	-	-
0.25	38.9121	39.1350	-	38.116
0.26	38.3850	-	-	-
0.3	34.9684	35.2318	36.40	34.829
0.4	24.2537	25.4709	25.296	23.858
0.5	15.8692	16.0858	16.43	15.720
0.6	10.4924	10.7410	11.29	10.431
0.7	7.1258	7.4862	-	7.101
0.74	6.1530	6.6072	-	6.139
0.8	4.9768	5.6512	5.31	4.978
0.8544	4.1421	4.1421	-	-
0.8631	4.0224	6.8976	-	-
0.8660	3.9846	7.623	-	-

We find that the maximum of the cross sections is at k = 0.23, which corresponds to a photon of wavelength 8406.3 Å, (using $\lambda = 911.267/\omega$ Å). As the momentum of the emitted electron, k, tends to zero, the photodetachment cross sections of the negative hydrogen ion tend to zero because the final state function is proportional to $j_1(kr)$ which goes to zero for as k tends to zero. Further, the cross section is directly proportional to k. Therefore, cross section is equal to zero at k = 0.0.

Ohmura and Ohmura [12], using the effective range theory and the loosely bound structure of hydrogen ion, obtained

$$\sigma = \frac{6.8475 \times 10^{-18} \gamma k^3}{(1 - \gamma\rho)(\gamma^2 + k^2)^3} \text{cm}^2 \tag{17}$$

In the above expression, γ = 0.2355883 is the square root of the binding energy and ρ = 2.646 $\pm$ 0.004 is the effective range. The maximum of these cross sections occurs at k = 0.236 or at 8195 Å which is close to the maximum of the cross sections obtained using the hybrid theory. Miyska at el. [13], using the R-matrix approach, have obtained accurate results for the photodetachment of the negative H ion. However, their results are given in form of curves and it is difficult to get accurate results for comparison. The experimental results [14,15] are also given in the form of curves and it is difficult to get accurate results for comparison. However, they appear to be close to the present results. The maximum is around 8000 Å, which is close to 8406.3 Å obtained using the hybrid theory. The results obtained using the hybrid theory and those obtained using Equation (17) are given in Figure 1. We find that the two sets of results are very close to each other.

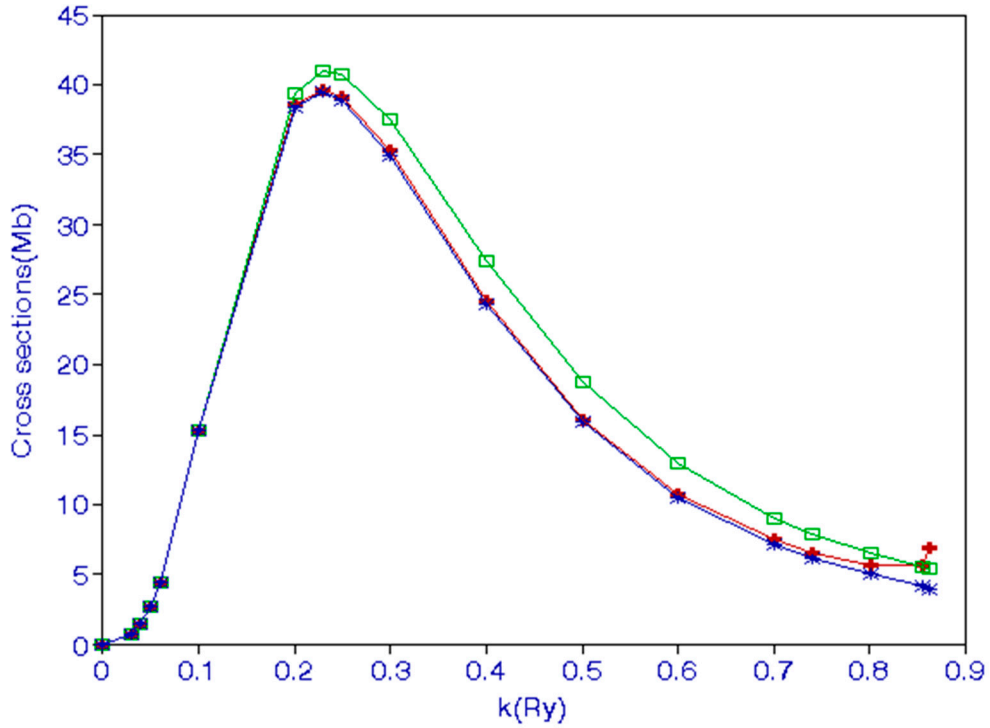

Figure 1. Photodetachment of a hydrogen negative ion. The lowest curve is obtained when only the long-range correlations in Equation (15) are included; the middle curve is obtained when the short-range and long-range correlations are included in Equation (15). The top curve is obtained for cross sections obtained by Ohmura and Ohmura using the effective range theory, Equation (17).

Similar calculations have been carried out for the photoionization of He and Li^+. The results have been compared with the results obtained in other calculations and also with the experimental results, the agreement is good. Cross sections for photoionization of He agree with those obtained using the R-matrix theory [16] and the experimental results [17,18]. These results are given in Table 2 and are also shown in Figure 2. All the three curves overlap. It is not possible to distinguish one curve from the other. This indicates that the hybrid theory gives results which are as accurate as those obtained using the R-matrix formulation, which is a very a versatile but is a very complicated theory. Photoabsorption in He played an important role in indicating the presence of resonances and in determining their positions and widths [19]. The line shape parameter q [20] is inversely proportional to the matrix element in the calculation of photoionization given in Equation (2). This parameter can be calculated accurately because the matrix element is known accurately. The matrix element appearing in the expression for q depends on the bound state wave function and the continuum function of the ejected electron in the photoionization cross section, and these functions can be obtained with very high accuracy.

It should be pointed out that these cross sections are finite as k goes to zero. In this case, the final continuum functions are Coulomb functions which behave like reciprocal of the square root of k. The k outside cancels with k inside the square of the matrix element giving finite cross sections as k goes to zero.

Yan et al. [21] using the accurate measurements at low energies and theoretical calculated results at high energies have calculated photoionization cross sections of He and H_2. Their interpolated results for He agree well with cross sections obtained using the hybrid theory given in Table 2. They have also calculated photoionization cross sections of H_2 as well as sum rules for He and H_2.

Table 2. Photoionization cross sections (Mb) for the ground state of He obtained with correlations.

k	Hybrid Theory [8]	R-Matrix [16]	Experiment Ref. [17]	Experiment Ref. [18]
0.1	7.3300	7.295	7.51	7.44
0.2	7.1544	7.115	7.28	7.13
0.3	6.8716	6.838	6.93	6.83
0.4	6.4951	6.474	6.49	6.46
0.5	6.0461	6.006	5.99	6.02
0.6	5.5925	5.535	5.46	5.55
0.7	5.0120	4.995	4.92	5.04
0.8	4.4740	4.482	4.38	4.51
0.9	3.9649	-	-	-
1.0	3.4654	3.476	3.38	3.48
1.1	3.0206	3.023	2.91	3.00
1.3	2.2561	2.271	2.17	2.19
1.4	1.9821	1.943	1.87	1.89
1.5	1.6817	-	-	-
1.6	1.6329	-	-	-

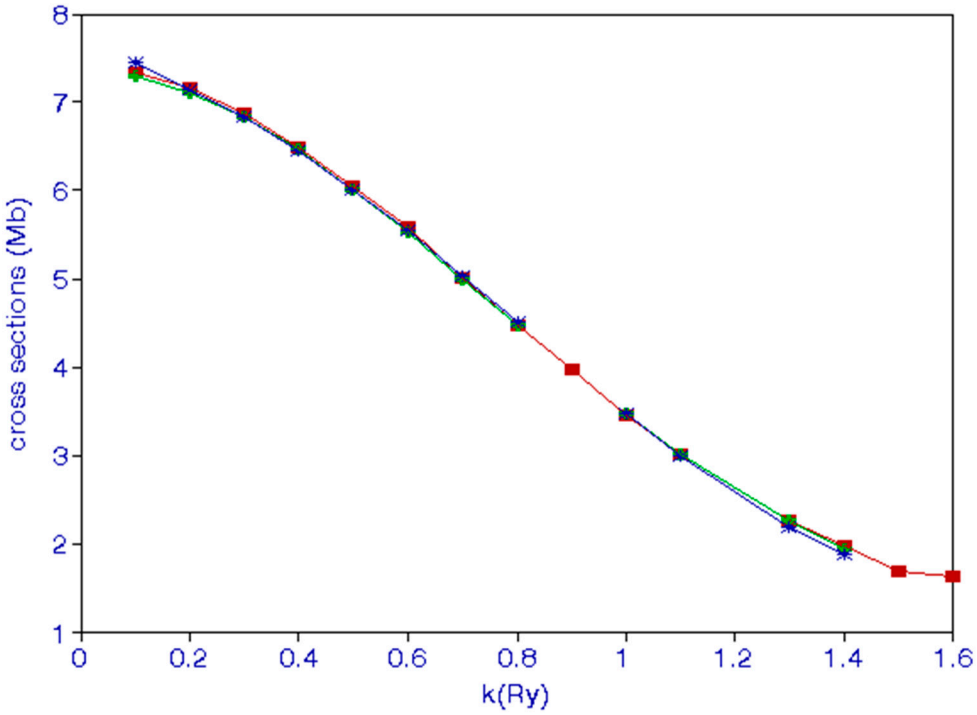

Figure 2. Photoionization of He. A comparison of cross sections calculated using the hybrid theory [8] and *R*-matrix approximation [16] with the experimental results [17,18] is shown.

Similar calculations [9] for photoionization of (1s2s) ^1S and ^3S states of He have been carried using the hybrid theory [8] with 455 terms in the bound state wave function. These results are shown in Table 3. The cross sections are compared with those obtained by Norcross [22], using the method of coupled equations for calculating the continuum functions. The results obtained using the hybrid theory are also compared with those of Jacobs [23], who also used pseudostates in the coupled equations.

Similar calculations [9] also have been carried for Li^+ using the hybrid theory with 165 terms for the ground state wave function. Calculations have also been carried out by the method of polarized orbits. The results obtained using the hybrid theory are given in Table 4 and they are compared with results of Bell and Kingston [10] and Daskhan and Ghosh [24]; the method of polarized orbitals [6] has been used in Refs. [10,24].

Table 3. Photoionization cross sections (Mb) for the metastable states of He.

(1s2s) ^1S State of He			
k	**Hybrid Theory [9]**	**Norcross [22]**	**Jacobs [23]**
0.1	8.7724	8.973	-
0.2	7.5894	7.344	-
0.3	6.0523	5.885	-
0.4	4.5403	4.595	-
0.5	3.2766	3.467	3.260
0.6	2.2123	2.515	2.357
0.7	1.6047	1.725	1.661
0.8	1.1230	1.104	1.141
0.9	0.7863	0.647	0.771
1.0	0.5474	0.360	0.521
1.1	0.3796	0.240	0.364
1.3	0.1858	-	0.212
1.4	0.1279	-	0.162
1.5	0.07001	-	0.090
(1s2s) ^3S state of He			
0.1	5.2629	4.749	-
0.2	5.0795	4.564	-
0.3	4.2004	4.112	-
0.4	3.4403	3.537	-
0.5	2.7189	2.912	-
0.6	2.1531	2.295	-
0.7	1.4564	1.733	-
0.8	1.3539	1.256	-
0.9	0.9728	0.885	-
1.0	0.6551	0.623	-
1.1	0.5577	0.463	-
1.2	0.3744	0.383	-
1.3	0.2898	0.347	-
1.5	0.2218	-	-

Table 4. Photoionization cross sections (Mb) of the ground state (1s1s) ^1S of $Li^{+\cdot}$.

k **(Ry)**	**Hybrid Theory, Ref. [8]**	**Ref. [10]**	**Ref. [24]**
1.6	1.1706	1.183	1.146
1.5	1.2768	1.297	1.248
1.4	1.3879	1.414	1.353
1.3	1.5035	1.533	1.459
1.2	1.6219	1.652	1.566
1.1	1.7396	1.770	1.674
1.0	1.8613	1.886	1.780
0.9	1.9792	1.998	1.885
0.8	2.0921	2.105	1.988
0.7	2.0005	2.206	2.087
0.6	2.2088	2.993	2.182
0.5	2.3870	2.384	2.271
0.4	2.4373	2.457	2.355
0.3	2.5231	2.520	2.432
0.2	2.5677	2.569	2.501

Photoionization cross sections of the metastable states of Li^+ ion have been calculated using the hybrid theory and 165 terms for the (1s2s) ^1S state and 120 terms for the (1s2s) ^3S state [9]. These results are shown in Table 5.

Table 5. Cross sections (Mb) for the metastable states of Li^+ ion.

K (Ry)	(1s2s) ^1S	(1s2s) ^3S
0.1	-	2.4456
0.2	2.5677	2.3780
0.3	2.5231	2.235
0.4	2.4622	2.0516
0.5	2.3869	1.8437
0.6	2.2998	1.6284
0.7	2.1999	1.4175
0.8	2.0925	1.2173
0.9	1.9789	1.0349
1.0	1.8605	0.8733
1.1	1.7414	0.7327
1.2	1.6219	0.6096
1.3	1.5037	0.5071
1.4	1.3886	0.4252
1.5	1.2777	0.3556
1.6	1.1716	0.2979
1.7	1.0712	0.2503
1.8	0.9770	0.2109
1.9	0.8892	0.1788
2.0	0.8079	0.1524
2.1	0.7332	0.1311
2.2	0.6649	0.1141
2.3	0.6034	0.1012
2.4	0.5488	0.0931
2.5	0.5025	0.0936

2. Radiative Attachment

Until this point, we have discussed the photodetachment process. However, the inverse process, namely, the radiative attachment is also possible. This process plays an important role in solar- and astrophysical problems. This is an important process, creating negative hydrogen ions which are important in understanding opacity of the solar system. The formation of the hydrogen molecule takes place through such processes:

$$e + H \rightarrow H^- + h\nu \tag{18}$$

$$H^- + H \rightarrow H_2 + e \tag{19}$$

Such recombination processes take place in the early Universe when the temperature of matter and radiation was close to a few thousand degrees. In Equations (18) and (19), H can be replaced by He^+ and Li^{2+} to form a He atom and Li^+ ion in the final state. The attachment cross section in terms of the photodetachment cross sections or photoionization cross section σ is given by

$$\sigma_a = \left(\frac{h\nu}{cp_e}\right)^2 \frac{g_f}{g_i}\sigma = \left(\frac{h\nu}{cp_e}\right)^2 \frac{1}{2mE}\frac{g_f}{g_i}\sigma \tag{20}$$

This relation follows from the principle of detailed balance. In Equation (20), $p_e = k$ is the incident electron momentum. The radiative-attachment cross sections are smaller than the photoabsorption cross sections. In Equation (20),

$$g_i = (2l_e + 1)(2S_e + 1)(2S_H + 1) = 3 \times 2 \times 2 = 12$$

and

$$g_f = (2 \times l_{h\nu} + 1)(2)(2S_{H^-} + 1) = 6(2S_{H^-} + 1)$$

The electron has an angular momentum = 1 = photon angular momentum, photon has two polarization directions, spin of the electron = 0.5 = spin of H, while the spin of the negative H^- = 0. Combining all these factors, we get g_i and g_f. These cross sections averaged over the Maxwellian velocity distribution $f(E)$ is given by

$$\alpha_R(T) = \langle \sigma_a v_e f(E) \rangle \tag{21}$$

The electron velocity is v_e, the recombination rate coefficient is given by

$$\alpha_R(T) = \left(\frac{2}{\pi}\right)^{0.5} \frac{c}{(mc^2 k_B T)^{1.5}} \frac{g_f}{g_i} \int dE(E+I)^2 \sigma e^{-E/k_B T} \tag{22}$$

$E = k^2$ is the energy of the electron in Equation (22), k_B is the Boltzmann constant, T is the electron temperature, and photon energy is $E = I + k^2$, where I is the threshold for photoabsorption. In Table 6, we give the recombination rates, averaged over the Maxwellian velocity distribution, at various temperature for the negative hydrogen ion, He, and Li^+. A comparison with R-matrix results is also given in Table 6.

Table 6. Recombination rate coefficients (cm^3/s) for (1s1s) state of H^-, He, and Li^+. A comparison with R-matrix results (interpolated) is also indicated.

T	$\alpha_R(T)\times 10^{15}$, H^-	$\alpha_R(T)\times 10^{13}$, He		$\alpha_R(T)\times 10^{11}$, Li^+
-	-	**Using Hybrid Theory Cross Sections Results**	**Using R-Matrix Cross Sections [25]**	-
1000	0.99	2.50	4.75	0.12
2000	1.28	2.30	3.43	1.04
5000	2.40	1.87	2.15	2.62
7000	2.82	1.66	1.79	2.92
10,000	3.20	1.45	1.48	3.03
12,000	3.37	1.35	1.36	3.02
15,000	3.56	1.23	1.22	2.95
17,000	3.65	1.17	1.19	2.89
20,000	3.75	1.10	1.08	2.79
22,000	3.79	1.05	1.04	2.73
25,000	3.83	0.99	0.99	2.63
30,000	3.83	0.92	0.93	2.49
35,000	3.77	0.87	0.89	2.36
40,000	3.67	0.82	0.86	2.25

The radiative rate coefficients for attachment to metastable states (1s2s) $^{1,3}S$ states of He and Li^+ are given in Table 7. A comparison of the results obtained using the hybrid theory with those obtained using the R-matrix formalism is also given in Table 7.

An extensive search to find the R-matrix calculations on recombination to Li ion failed to find any results. It seems such a calculation has not been carried out.

Nahar [25] has carried out R-matrix calculations of photoionization of the helium atom and recombination rate coefficients. Her photoionization results have been discussed above. The agreement between the cross sections obtained using the hybrid theory and R-matrix, along with the experimental results, is very good. The recombination rate coefficients to the ground state using the hybrid theory given in Table 6 agree with the results obtained using the R-matrix theory. The results for metastable states are indicated in Table 7. The agreement of the rate coefficients for the metastable states is quite good. This is surprising because the photoionization cross sections for metastable states obtained using the hybrid theory agree well with those obtained using the close-coupling approximation [22,23].

The reason that the method of polarized orbitals works well for atoms as well as for ions to provide accurate results for photoabsorption cross sections is the fact that the polarized target function depends on the nuclear charge Z only, as indicated in Equation (13).

Table 7. Recombination rate coefficients (cm^3/s) of the metastable states of He and Li^+, and comparison with the R-matrix results (interpolated).

-	He				Li^+	
-	^3S		^1S		^3S	^1S
-	Hybrid	R-Matrix	Hybrid	R-Matrix	Hybrid	Hybrid
T	$\alpha_R(T)\times10^{14}$		$\alpha_R(T)\times10^{15}$		$\alpha_R(T)\times10^{14}$	$\alpha_R(T)\times10^{14}$
1000	2.13	4.33	8.27	17.13	4.68	2.99
2000	2.08	3.20	7.97	12.55	4.47	2.87
5000	1.71	2.05	7.30	7.85	3.48	2.37
7000	1.56	1.71	5.71	6.43	3.09	2.03
10,000	1.40	1.39	5.05	5.12	2.68	1.78
12,000	1.32	1.26	4.73	4.54	2.49	1.66
15,000	1.23	1.11	4.35	3.93	2.26	1.52
17,000	1.18	1.04	4.15	3.64	2.14	1.45
20,000	1.12	0.97	3.90	3.33	1.98	1.36
22,000	1.09	0.94	3.75	3.19	1.90	1.31
25,000	1.04	0.91	3.57	3.05	1.79	1.24
30,000	0.98	0.90	3.31	2.97	1.64	1.15
35,000	0.93	0.92	3.10	3.03	1.52	1.08
40,000	0.89	0.97	2.93	3.18	3.14	1.02

3. Photoejection with Excitation

Up to now we have considered photoabsorption when the remaining atom or ion is left in the ground state. However, it is possible to leave the remaining atom or ion in an excited state [26]. For example, in the photoionization process

$$h\nu + He \rightarrow He^+ + e \tag{23}$$

In the above equation, ionized helium can be in the excited 2^2S or 2^2P states. When the remaining atom or ion is in the 2^2P state, there is a possibility of emission of Lyman-α radiation of 304 Å, as in the photodetachment of the negative hydrogen ion or photoabsorption. The outgoing photoelectron can be in the angular momentum l_f = 0 or 2 when the resulting state is in ^2P state and l_f = 1 when the resultant state is ^2S state. Similar processes can take place when the targets are H^-, Li^+, Be^{2+}, and C^{4+}.The cross section in the dipole approximation is given by

$$= \frac{4\pi\alpha k\omega}{3(2l_i+1)}(|M_0|^2 + |M_2|^2) \tag{24}$$

for ^2P states and

$$= \frac{4\pi\alpha\omega}{3(2l_i+1)}|M_1|^2 \tag{25}$$

for ^2S states. The matrix M is defined as

$$M_{l_f} = (2l_f+1)^{0.5}|\langle\Psi_f|z_1+z_2|\Phi_i\rangle| \tag{26}$$

The continuum functions are calculated in the exchange approximation (cf. Equation (5)). Table 8 gives the ratios $R_1 = \sigma(2^2S)/\sigma(1^2S)$ and $R_2 = [\sigma(2^2S) + \sigma(2^2P)]/\sigma(1^2S)$ for the negative hydrogen ion. *He* and Li^{2+}. Komninos and Nicolaides [27] have calculated ratios of leaving the He ion in 2p and 2s states using the K-matrix theory. Jacobs and Burke [28] have also calculated these ratios using the close-coupling approximation. The agreement with the results of [27,28] is not good because the continuum functions are calculated in the exchange approximation, instead of using the hybrid theory. However,

the calculations are much easier than using other approximations. The simpler approach might not give definitive results but is helpful in understanding various processes.

Table 8. Ratios R_1 and R_2.

k	R_1	R_2
-	H^-	
0.1	1.1760 (−4)	8.1873 (−2)
0.2	3.9946 (−4)	4.4460 (−2)
0.3	2.2783 (−3)	4.9332 (−2)
0.4	1.3944 (−2)	6.1779 (−2)
0.5	6.4958 (−2)	1.0498 (−1)
0.6	1.6743 (−1)	2.0920 (−1)
0.7	2.6673 (−1)	3.2210 (−1)
0.8	3.3490 (−1)	3.9742 (−1)
-	He	
0.1	8.0146 (−3)	1.2794 (−2)
0.2	8.6667 (−3)	1.3318 (−2)
0.3	9.6384 (−3)	1.4112 (−1)
0.4	1.0774 (−2)	1.5065 (−1)
0.5	1.1935 (−2)	1.6097 (−2)
0.6	1.3075 (−2)	1.7206 (−2)
0.7	1.4252 (−2)	1.8497 (−2)
0.8	1.5551 (−2)	2.0062 (−2)
-	Li^+	
0.2	4.9346 (−3)	6.4426 (−3)
0.3	4.9889 (−3)	6.5041 (−3)
0.4	5.0594 (−3)	6.5849 (−3)
0.5	5.1422 (−3)	6.6814 (−2)
0.6	4.0317 (−3)	5.2310 (−3)
0.7	5.3781 (−3)	6.9693 (−3)
0.8	5.5344 (−3)	7.1657 (−3)
0.9	5.7203 (−3)	7.4081 (−3)
1.0	5.9438 (−3)	7.6979 (−3)
1.1	6.2085 (−3)	8.0436 (−3)
1.2	6.5170 (−3)	8.4476 (−3)
1.3	6.8761 (−3)	8.9126 (−3)
1.4	7.2914 (−3)	9.4507 (−3)
1.5	7.7664 (−3)	1.0062 (−2)
1.6	8.3090 (−3)	1.0753 (−2)

The radiative rate coefficients averaged over the Maxwellian velocity distribution are given in Table 9.

Table 9. Recombination rate coefficients (cm^3/s) to (1s1s) ^1S state from ^2S and ^2P states.

T	$\alpha_R \times 10^{16}$, H^-	$\alpha_R \times 10^{16}$, He	$\alpha_R \times 10^{16}$, H^-	$\alpha_R \times 10^{16}$, He
-	Final State is ^2S		Final State is ^2P	
2000	4.36 (−3)	19.3	0.75	33.7
4000	2.86 (−2)	16.8	1.00	25.0
5000	5.83 (−2)	15.9	1.10	22.1
7000	1.73 (−1)	14.5	1.24	17.9
10,000	5.07 (−1)	13.2	1.35	14.0
12,000	8.30 (−1)	12.6	1.38	12.2
15,000	1.43	11.8	1.39	10.2
17,000	1.93	11.4	1.38	9.25
20,000	2.59	10.9	1.36	8.07

Table 9. *Cont.*

T	$\alpha_R \times 10^{16}$, H^-	$\alpha_R \times 10^{16}$, He	$\alpha_R \times 10^{16}$, H^-	$\alpha_R \times 10^{16}$, He
-	Final State is ^2S		Final State is ^2P	
22,000	3.17	10.7	1.34	7.43
25,000	3.89	10.3	1.30	6.64
30,000	4.97	9.98	1.24	5.64
35,000	5.86	9.55	1.18	4.89
40,000	6.55	9.28	1.12	4.31
45,000	7.06	9.06	1.06	3.86
50,000	7.43	8.88	1.00	3.48
60,000	7.81	8.62	0.904	2.91
70,000	7.88	8.42	0.818	2.50
80,000	7.76	8.26	0.742	2.18
90,000	7.53	8.11	0.676	1.93
100,000	7.25	7.97	0.619	1.73
200,000	4.48	6.38	0.307	0.82
300,000	2.96	4.94	0.189	0.511

4. Photoionization of Lithium and Sodium

Until this point, we discussed photoabsorption where the continuum functions were calculated using hybrid theory. However, we have some calculations mentioned above where the method of polarized orbitals was used. There are other calculations like photoionization of lithium [29] where the method of polarized orbitals was used. Cross sections for this process are given in Table 10.

Table 10. Photoionization cross sections (10^{-18} cm^2).

k	Cross Section	K	Cross Section
0.10	1.601	0.80	0.905
0.20	1.672	0.90	0.724
0.30	1.709	1.00	0.574
0.35	1.697	1.20	0.355
0.40	1.660	1.40	0.219
0.50	1.521	1.60	0.136
0.54	1.427	1.80	0.087
0.60	1.324	1.90	0.069
0.70	1.110	-	-

Similar calculations [30] have been carried out for the photoionization of sodium atoms. These results are given in Table 11 and are compared with the close-coupling results of Butler and Mendoza [31]. Cross sections at low energies agree fairly well with those obtained using the close-coupling approximation.

Table 11. Photoionization cross sections (10^{-20} cm^2) of Na atoms.

k	Pol. Orb. Approx. [30]	Close-Coupling Approx. [31]
0.0	8.419	8.496
0.1	5.748	5.390
0.2	1.228	1.142
0.3	0.319	0.264
0.4	3.536	3.513
0.5	7.832	7.773
0.6	11.111	11.416
0.7	12.627	13.411
0.8	12.815	13.740
0.9	12.157	12.957
1.0	11.047	12.102

Table 11. *Cont.*

k	Pol. Orb. Approx. [30]	Close-Coupling Approx. [31]
1.1	9.934	12.102
1.2	8.602	-
1.3	7.714	-
1.4	6.893	-
1.5	6.134	-
1.6	5.361	-
1.7	4.843	-
1.8	4.392	-
1.9	3.905	-
2.0	3.507	-

5. Photodetachment of $^3P^e$ State of Negative Hydrogen Ion

It is well known that the negative hydrogen ion has only one bound state. However, there is another bound triplet $(2p2p)P$ state of even parity, which is not well known. The bound state function has been calculated using Hylleraas type functions [32], where the energy of the state is given as $-0.2506536415\ Rm$, and Rm is the reduced Rydberg. This photodetachment process is similar to photoejection mentioned above in Equation (22). The continuum functions were calculated using the 1s-2s-2p close coupling approximation [33]. Cross sections are given in Table 12.

Table 12. Cross sections (cm^2) for the photodetachment of the $^3P^e$ state of a negative hydrogen ion.

Photon Energy (Ry)	Final State Is (2s)	Final State Is (2p)
0.002	8.74 (−17)	3.99 (−16)
0.004	6.67 (−17)	4.01 (−16)
0.006	4.61 (−17)	3.03 (−16)
0.008	3.52 (−17)	2.43 (−16)
0.010	2.90 (−17)	2.18 (−16)
0.014	2.16 (−17)	1.99 (−16)
0.018	1.69 (−17)	1.76 (−16)
0.022	1.38 (−17)	1.50 (−16)
0.026	1.16 (−17)	1.27 (−16)
0.030	1.01 (−17)	1.10 (−16)
0.040	7.93 (−18)	8.33 (−17)
0.050	6.81 (−18)	6.79 (−17)
0.150	2.64 (−18)	1.69 (−17)
0.250	8.63 (−18)	6.37 (−18)

Radiative attachment

$$e + H(2s) \rightarrow H(2\,^3P^e) + h\nu \tag{27}$$

$$e + H(2p) \rightarrow H(2^3P^e) + h\nu \tag{28}$$

These two processes are important sources of infrared emission. The radiative attachment cross sections are given in Ref. [30].

6. Photodetachment of Negative Positronum Ion

Photodetachment of the negative positronium ion is very much like the photodetachment of a negative hydrogen ion. It is indicated by

$$h\nu + Ps^- \rightarrow e^- + Ps \tag{29}$$

This process also contributes to the opacity of the Sun and the stellar atmosphere. The

binding energy of the positronium ion has been calculated by Bhatia and Drachman [34]. Following Ohmura and Ohmura [12], we write the wave function of the positronium ion as

$$\Phi(R_j, r_k) = C\frac{e^{-\gamma R_j}}{R_j}\phi(r_k) \tag{30}$$

The constant C is determined using the exact wave function given in Ref. [34], where $\frac{3\gamma^2}{2}$ = binding energy = 0.024010113. We use plane waves for the scattering function [35]. The expression for the cross section is given in Equation (31). The cross section is the same for the process obtained by the charge conjugation of the process indicated in Equation (29). The cross section [35] is given by

$$\sigma = 1.32 \times 10^{-18}\frac{k^3}{(k^2+\gamma^2)^3}\text{cm}^2 \tag{31}$$

In Table 13, cross sections for the photodetachment are given, and they are also indicated in Figure 3.

Table 13. Photodetachment. Cross sections (cm^2).

Photon Energy (Ry)	Cross Section
0.26	1.58 (−17)
0.22	1.98 (−17)
0.20	2.41 (−17)
0.16	2.97 (−17)
0.13	3.81 (−17)
0.12	4.17 (−17)
0.11	4.59 (−17)
0.10	5.08 (−17)
0.08	6.27 (−17)
0.07	6.97 (−17)
0.065	7.33 (−17)
0.060	7.67 (−17)
0.05	8.13 (−17)
0.04	7.66 (−17)
0.03	4.16 (−17)

We can use the Thomas–Reiche–Kuhn sum rule to judge the accuracy of our calculation. The sum rule is given by

$$S_{-1} = \frac{1}{2\pi^2\alpha a_0^2}\int_0^{\lambda_0}\frac{d\lambda}{\lambda}\sigma(\lambda) = \frac{8}{27}\langle(\vec{r}_1+\vec{r}_2)^2\rangle = \frac{8}{27}(4\langle r_1^2\rangle - \langle r_{12}^2\rangle) \tag{32}$$

In the above equation, λ_0 is the threshold wave length for the photodetachment of the negative positronium ion. The expectation values of $\langle r_1^2\rangle$ and $\langle r_{12}^2\rangle$ have been calculated using the exact wave function of the positronium ion [34]. The left-hand side of Equation (32) is equal to 31.7 and the right-hand side is equal to 29.775. This shows that our cross section using the approximate wave functions exceed by 6.5%. This is confirmed by Ward et al. [36], who have carried out accurate calculations using accurate initial state wave function having 95 linear parameters of Ps^- and continuum functions were obtained using the Kohn variational principle with 220 linear parameters. Their results for the cross sections are lower (cf. figure in their paper) than those obtained in Ref. [35].

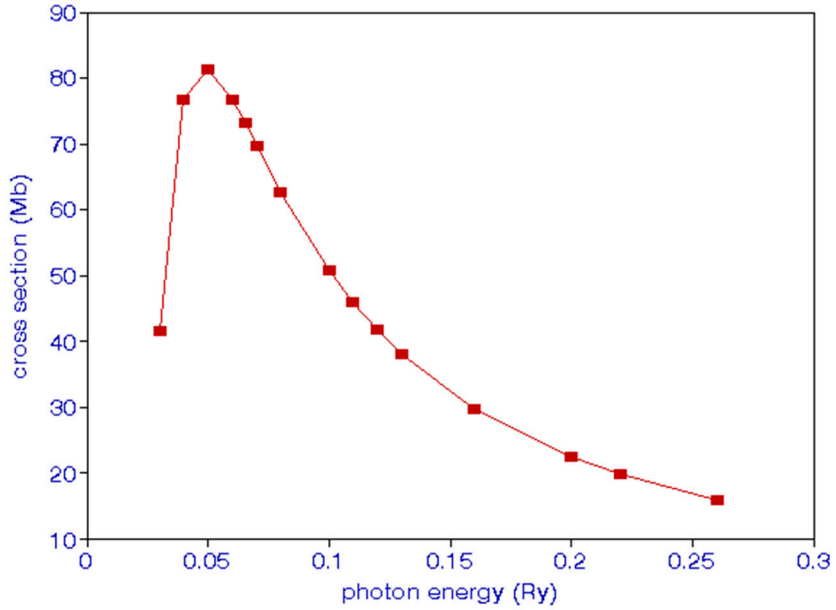

Figure 3. (Color online). Photodetachment cross sections (Mb) of Ps^- vs. photon energy (Ry).

This calculation [35] has been extended to the photodetachment of the positronim ion when the positronium atom is left in nP states, n = 2, 3, 4, 5, 6, and 7 [37]. The ^2P state can decay into ^1S state which would correspond to Lyman-α Ps-radiation, just like 1216 Å radiation which has been observed from the center of galaxy [38], where it is due to a transition from ^2P to ^1S in a hydrogen atom. The photodetachment cross sections to various excited states are given below:

$$\begin{aligned}\sigma(2p) &= 164.492C(k)\\ \sigma(3p) &= 26.3782C(k)\\ \sigma(4p) &= 9.1664C(k)\\ \sigma(5p) &= 4.3038C(k)\\ \sigma(6p) &= 2.3764C(k)\\ \sigma(7p) &= 0.2675C(k)\end{aligned}$$

where,

$$C(k) = \frac{10^{-20}k}{(\gamma^2 + k^2)}\text{cm}^2 \tag{33}$$

Similar calculations can be carried out for leaving the positronium atom in ns states, n = 2 to 7. The transition from the 2s state to 1s state would be with the emission of 2 photons just like that in the case of a hydrogen atom.

We have discussed photoionization and photoabsorption for various systems using the expression for the cross section given in Equation (2). The derivation of this formula in Equation (2) is given in [39] (repeated in the Appendix A). In this article, photoionization cross sections of the (1s1s ^1S), (1s2s $^{1,3}S$), (1s3s ^3S) states of Be^{2+}, C^{4+}, and O^{6+}, along with radiative recombination rate coefficients at various electron temperatures, are given. Fitting formulae for photoionization cross sections are also given in [39].

Until this point, we have mostly mentioned two-electron systems and we have given cross sections using the exchange approximation, method of polarized orbitals, plane-wave approximation, *R-matrix* formulation, and hybrid theory. There are other calculations like coupled cluster study of photoionization by Tenoril et al. [40]. They use an asymptotic Lanczos algorithm to calculated photoionization and photodetachment cross sections of of He and give results in the form of a curve. It is difficult to get meaningful results for a comparison. However, they do give the sum rule S(0) = 1.999 for He, which is close to the exact value equal to 2, the number of electrons in the He atom, indicating the accuracy

of their calculation. The exterior complex scaling has been used by Andric et al. [41] to calculate photoionization cross section of positive HCl ion. Measurements of photodetachment cross sections of Li^-, Be^-, and B^- have been carried out using interacting beams by Pegg [42]. Photoionization cross sections of excited states of CO, N_2, and H_2O have been calculated by Ruberti et al. [43] using the many-electron Green's function approach. In a simple system like a hydrogen atom, Broad and Reinhardt [44] used L^2 basis to calculate photoionization of a hydrogen atom in the energy range 1.002 to 3.50 Rydberg; their results are given in Table 14. Their results appear close to those given by Joachain [45] in his book and also to the result 0.225 a_0^2 at the threshold. These cross sections obtained using L^2 basis are higher than those obtained using the R-matrix approach. Perhaps, there is possibility of improving the L^2 basis approach. It is very important to try other approximations in addition to the R-matrix approach.

Table 14. Photoionization cross sections (a_0^2) of a hydrogen atom.

Photon Energy (Ry)	Cross Section	*R*-Matrix Cross Section [a]
1.002	0.4478	-
1.500	0.1494	0.0747
2.000	0.0666	0.03327
2.500	0.0350	0.01438
3.000	0.0206	0.01045
3.500	0.0130	0.00654

[a] These cross sections calculated by S. N. Nahar are given in NORAD Atomic-Data.

Very recently, Nahar [46] has carried out very detailed and accurate calculations of photoionization cross sections and electron-ion recombination of $n = 1$ to very high n values of hydrogenic ions. Since hydrogen is very abundant in the universe, the results of this calculation are of immense importance in applications to solar- and astrophysics.

Paul and Ho [47] have calculated cross sections of H in the presence of Debye potential, while Kar and Ho [48] have calculated cross sections of the hydrogen negative ion in the Debye potential. Sahoo and Ho [49] have also calculated photoionization cross sections of Li and Na in the presence of the Debye potential. They find that in the presence of a Debye potential, the maximum of the photodetachment cross section of the negative ions moves to higher wave lengths as the Debye length decreases, making the plasma dense. The plasma is least dense when the Debye length is infinite.

7. Opacity

Opacity implies the loss of photons as in the photoabsorption indicated in Equations (1) and (29). We know the photodetachment cross sections of the negative hydrogen ion and of the positronium ion, we can compare their contributions to the opacity of the atmosphere of the Sun and the interstellar medium provided we include the free-free transitions:

$$h\nu + e + H \rightarrow e + H \tag{34}$$

$$h\nu + e + Ps \rightarrow e + Ps \tag{35}$$

In these processes the electron with energy k_0^2 absorbs an energy $h\nu$ of a photon in the initial state and the final energy of the electron is k^2, the change in energy is $h\nu = \Delta k^2 = |k_0^2 - k^2|$. The same kind of processes take place when the electrons in Equations (34) and (35) are replaced by positrons. The formula for free-free transitions has been given by Chandrasekhar and Breen [50]. Positrons had not been considered earlier and they contribute substantially, as indicated in Table 15, where a few values of cross sections are given at T = 6300 K.

Table 15. Comparison of bound-free (σ_{bf}) and free-free (σ_{ff}) cross sections (cm^2) for electrons and positrons, T = 6300 K.

$h\nu$ (Ry)	Electrons			Positrons		
-	σ_{bf}	σ_{ff}	σ_{bf}+σ_{ff}	σ_{bf}	σ_{ff}	σ_{bf}+σ_{ff}
0.26	2.26 (−17)	4.28 (−20)	2.27 (−17)	8.61 (−18)	4.14 (−21)	8.61 (−18)
0.24	2.47 (−17)	4.94 (−20)	2.47 (−17)	9.58 (−18)	4.74 (−21)	9.58 (−18)
0.22	2.70 (−17)	5.81 (−20)	2.70 (−17)	1.08 (−17)	3.49 (−21)	1.08 (−17)
0.20	2.96 (−17)	6.95 (−20)	2.96 (−17)	1.22 (−17)	6.45 (−21)	1.22 (−17)
0.18	3.25 (−17)	8.53 (−20)	3.25 (−17)	1.39 (−17)	7.71 (−2 1)	1.39 (−17)
0.16	3.56 (−17)	1.07 (−19)	3.57 (−17)	1.62 (−17)	9.49 (−21)	1.62 (−17)
0.14	3.87 (−17)	1.39 (−19)	3.88 (−17)	1.90 (−17)	1.19 (−20)	1.90 (−17)
0.12	4.15 (−17)	1.88 (−19)	4.17 (−17)	3.17 (−17)	1.56 (−20)	3.17 (−17)
0.10	4.13 (−17)	2.69 (−19)	4.16 (−17)	4.17 (−17)	2.15 (−20)	4.17 (−17)
0.08	3.50 (−17)	4.20 (−19)	3.35 (17)	3.42 (−17)	3.20 (−20)	3.42 (−17)
0.06	7.05 (−18)	7.45 (−19)	7.80 (−18)	8.96 (−17)	5.38 (−20)	8.97 (−17)
0.04	0.0 [a]	1.68 (−18)	1.68 (−18)	1.65 (−16)	1.13 (−19)	1.65 (−16)
0.03	0.00	2.99 (−18)	2.99 (−18)	2.53 (−16)	1.96 (−19)	2.53 (−16)
0.02	0.00	6.74 (−18)	6.74 (−18)	4.64 (−16)	4.30 (−19)	4.64 (−16)
0.01	0.00	2.70 (−17)	2.70 (−17)	1.30 (−15)	1.68 (−15)	1.30 (−15)
0.005	0.00	1.08 (−16)	1.08 (−16)	3.63 (−15)	6.72 (−15)	3.64 (−15)
0.003	0.00	3.00 (−16)	3.00 (−16)	7.69 (−15)	1.87 (−17)	7.71 (−15)
0.001	0.00	2.70 (−15)	2.70 (−15)	3.55 (−14)	1.68 (−16)	3.57 (−14)

[a] Photon energy less than 0.055 (Ry) is not sufficient for photodetachment.

In Figure 4, we give the total (detachment plus free-free) electron and positron cross sections. We find that the positron contribution is substantial and should be taken into account in the opacity calculations.

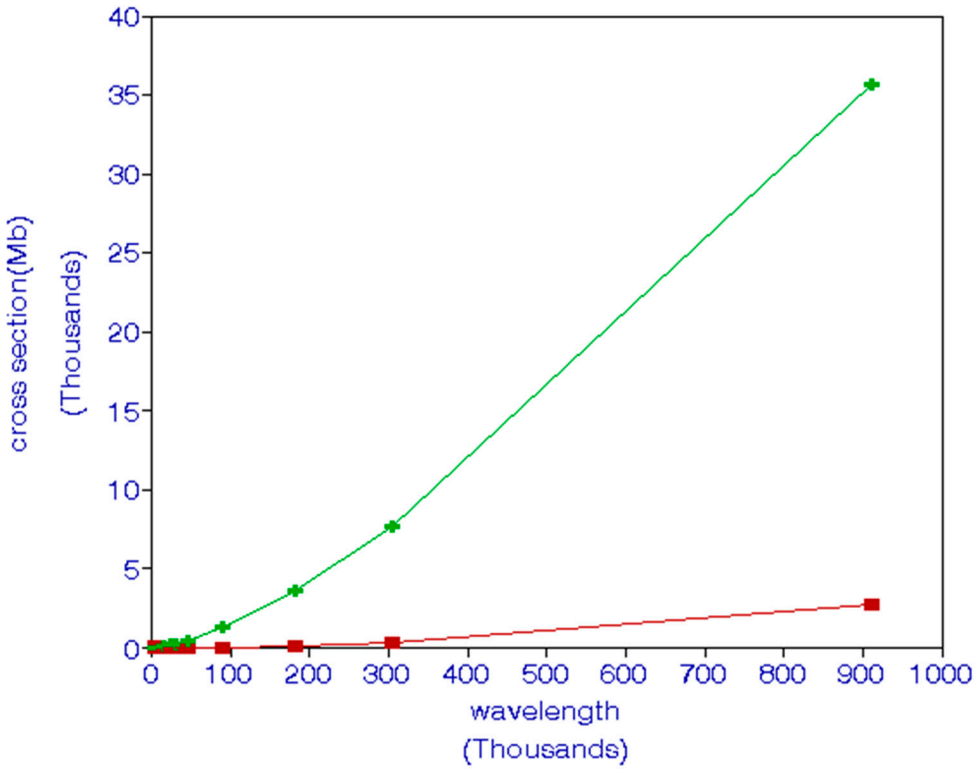

Figure 4. (Color online). The top curve refers to positron cross sections (Mb), while the lower curve refers to electron cross sections (Mb). Wavelengths are in units of Å.

Similarly, photoionization of other atoms and ions and free-free transitions contribute to opacity. However, hydrogen is the most abundant atom in the universe compared to other atoms and ions, whose concentrations decrease as Z, the nuclear charge, increases.

8. Conclusions

Here we described the photoabsorption process of two-electron systems for which scattering functions are required. There are various approaches to calculate continuum functions. We also described calculations in which we have used the exchange approximation, method of polarized orbitals, hybrid theory, close-coupling approximation, and R-matrix formalism. Further, we have mentioned photoabsorption cross sections of various molecules and sum rules. Cross sections were calculated using the coupled cluster formalism, which uses the asymptotic Lanczos algorithm, complex exterior scaling, and L^2 basis. These methods are briefly mentioned. Cross sections were compared with those obtained in other calculations and also with the experimental results. The photodetachment cross sections of the negative positronium ion, Ps^-, were calculated using the Ohmura and Ohmura approximation for the bound state and the plane-wave approximation for the final continuum state wave function. For a long time, it was thought that only processes involving electrons contribute to the opacity of the Sun and the interstellar medium. However, positrons do exist in many regions of the Sun and the interstellar medium [51]. Therefore, it is necessary to consider positrons in calculations of opacity. We have indicated in Table 15 that not only electrons but positrons also contribute substantially to the opacity of the Sun and of the interstellar medium.

Since the observation of the photoionization process in metals by Lenard [52] in 1902, there have been many experiments to observe photoionization in atoms, ions, and molecules and theoretical developments to calculate cross sections for this process. We have mentioned a few of the experiments and theoretical approaches.

Funding: This research work received no funding.

Institutional Review Board Statement: Not applicable.

Informed Consent Statement: Not applicable.

Data Availability Statement: There is no external data for this article.

Conflicts of Interest: The author declares no conflict of interest.

Appendix A

We briefly derive the photoionization formula for the hydrogen atom.

Photoionization is given by

$$h\nu + H \rightarrow H^+ + e \tag{A1}$$

The interaction Hamiltonian is given by

$$H' = -\frac{e}{2mc}(\vec{A}\cdot\vec{p} + \vec{p}\cdot\vec{A}) = -\frac{e}{mc}\vec{A}\cdot\vec{p} \tag{A2}$$

In the above equation, $\vec{A}$ is the vector potential and $\vec{p}$ is the electron momentum. The vector potential satisfies the condition $div\vec{A} = 0$ and it is represented by

$$\vec{A} = A_0\vec{\varepsilon}e^{i\vec{k}\cdot\vec{r}} \tag{A3}$$

In the above equation $\vec{k}$ is the photon momentum which in magnitude is less than the radius of the atom, which implies that the exponential factor can be taken as equal to 1.0. This is called the dipole approximation and $\vec{\varepsilon}$ is the polarization direction, perpendicular to

the z-axis, the incident photon direction. There are two polarization directions. However, for the derivation we need to consider only one of them and we can consider the polarization in the direction of the x-axis. The density of states is given by

$$\rho(k) = \frac{mk}{(2\pi)^3\hbar^2}\sin(\theta)d\theta d\varphi \tag{A4}$$

Here θ is the angle between $\vec{k}$ and the photon direction. The incident flux is given by

$$\frac{\omega^2 A_0^2}{2\pi c(\hbar\omega)} = \frac{\omega A_0^2}{2\pi\hbar c} \tag{A5}$$

The electron momentum satisfies the commutation relation

$$\langle\vec{p}\rangle = m\frac{d\vec{r}}{dt} = m\langle\frac{1}{i\hbar}[H,\vec{r}]\rangle = \frac{mE}{i\hbar}\hbar\omega\langle\vec{r}\rangle \tag{A6}$$

Therefore,

$$\langle H\prime\rangle = -\frac{e}{mc}\langle\vec{A}\cdot\vec{p}\rangle = -\frac{e\omega A_0}{ic}\langle\vec{\varepsilon}\cdot\vec{r}\rangle \tag{A7}$$

The transition probability is given by

$$\omega_p = \frac{2\pi}{\hbar}\rho(k)|\langle H\prime\rangle|^2 = \frac{2\pi}{\hbar}\rho(k)\frac{e^2\omega^2A_0^2}{c^2}|\langle\vec{\varepsilon}\cdot\vec{r}\rangle|^2 \tag{A8}$$

Therefore, the differential cross section is given by

$$\sigma(\theta,\varphi)\sin(\theta)d\theta d\varphi = \frac{\omega_p}{Flux} \tag{A9}$$

This gives

$$\sigma(\theta,\varphi) = \frac{2\pi}{\hbar}\frac{mk}{(2\pi)^3\hbar^2}\frac{e^2\omega^2}{c^2}\frac{A_0^2\left|\left\langle\vec{\varepsilon}\cdot\vec{r}\right\rangle\right|_2(2\pi\hbar c)}{\omega A_0^2} \tag{A10}$$

Since

$$\vec{\varepsilon}\cdot\vec{r} = (\vec{\varepsilon}\cdot\hat{k})(\hat{k}\cdot\vec{r}) = \sin(\theta)\cos(\varphi)(\hat{k}\cdot\vec{r}) \tag{A11}$$

$$\sigma(\theta,\varphi)\sin(\theta)d\theta d\varphi = \frac{mke^2\hbar\omega}{2\pi\hbar^3c}|\langle\hat{k}\cdot\vec{r}\rangle|^2\sin^3(\theta)\cos^2(\varphi)d\theta d\varphi \tag{A12}$$

Using $\int\sin^3(\theta)\cos(\varphi)^2d\theta d\varphi = \frac{4\pi}{3}$, we get the total cross section

$$\sigma = \frac{2mk}{\hbar^2}\frac{e^2}{\hbar c}\hbar\omega\frac{|\langle\hat{k}\cdot\vec{r}\rangle|^2}{3} \tag{A13}$$

where, $\frac{2m}{\hbar^2} = \frac{1}{1Ry\cdot a_0^2}$ and $\frac{e^2}{\hbar c} = \alpha$, the fine-structure constant, we get, using $\hbar\omega = I + k^2$

$$\sigma = k\alpha(I+k^2)|\langle\hat{k}\cdot\vec{r}\rangle|^2/3 \tag{A14}$$

The cross section given above is in the units of a_0^2, I and k^2 are in Ry units.

Since the normalization is a plane-wave normalization, the scattering function has a normalization

$$(4\pi(2l_f+1))^{0.5} \tag{A15}$$

Here $l_f = 1$ and

$$\hat{k}\cdot\vec{r} = r\cos(\theta_1) = z \tag{A16}$$

We get

$$\sigma(a_0^2) = 4\pi\alpha k(I + k^2)\langle z\rangle^2 \tag{A17}$$

Since there is no φ dependence because the scattering functions and bound state functions are functions of angle θ_1, x and y components do not contribute because, in Equation (4), only the magnetic quantum $m = 0$ is being considered, x corresponds to $m = 1$ and y corresponds to $m = -1$. We get

$$\sigma(a_0^2) = 4\pi\alpha k(I + k^2)\langle z\rangle^2 \tag{A18}$$

This formula can be generalized to more than one electron, as indicated in Equation (2). We have considered polarization direction in x-axis only. We could also add to (A11) the polarization in the y-direction but then we would have to average the result.

References

1. Hoffman, B. *The Strange Story of the Quantum*; Dover Publications: Mineola, NY, USA, 1947; p. 13.
2. Compton, A.H. A Quantum Theory of the Scattering of X-rays by Light Elements. *Phys. Rev.* **1923**, *21*, 483–502. [CrossRef]
3. Bothe, W.; Geiger, H. Uber das Wesen des Compton effects ein experimenteller Breitrag Theorie der Strahlung. *Z. Phys.* **1923**, *21*, 152.
4. Wildt, R. Electron Affinity in Astrophysics. *Astrophys. J.* **1939**, *89*, 295–301. [CrossRef]
5. Morse, P.M.; Allis, W.P. The Effect of Exchange on the Scattering of Slow Electrons from Atoms. *Phys. Rev.* **1933**, *44*, 269–276. [CrossRef]
6. Temkin, A. A Note on the Scattering of Electrons from Atomic Hydrogen. *Phys. Rev.* **1959**, *116*, 358–363. [CrossRef]
7. Sloan, I.H. The method of polarized orbitals for the elastic scattering of slow electrons by ionized helium and atomic hydrogen. *Proc. R. Soc. Lond. Ser. A Math. Phys. Sci.* **1961**, *281*, 151–163.
8. Bhatia, A.K. Hybrid theory of electron-hydrogen elastic scattering. *Phys. Rev. A* **2007**, *75*, 032713. [CrossRef]
9. Bhatia, A.K. Hybrid theory of *P*-wave electron-Li^{2+} elastic scattering and photoabsorption in two-electron systems. *Phys. Rev. A* **2013**, *87*, 042705. [CrossRef]
10. Bell, K.L.; Kingston, A.E. Photoionization of Li^+. *Proc. Phys. Soc.* **1967**, *90*, 337–342. [CrossRef]
11. Wishart, A.W. The bound-free photodetachment of H^-. *J. Phys. B* **1979**, *12*, 3511. [CrossRef]
12. Ohmura, T.; Ohmura, H. Electron-Hydrogen Scattering at Low Energies. *Phys. Rev.* **1960**, *118*, 154–157. [CrossRef]
13. Miyake, S.; Stancil, P.C.; Sadeghpour, H.R.; Dalgarno, A.; McLaughlin, B.M.; Forrey, R.C. Resonant H^- Photodetachment Enhanced Photodestruction and Consequences for Radiative Feedback. *Astrophys. J. Lett.* **2010**, *709*, L168–L171. [CrossRef]
14. Branscomb, L.M.; Smith, S.J. Experimental Cross Sections for Photodetachment of Electrons from H^- and D^-. *Phys. Rev.* **1955**, *98*, 1028. [CrossRef]
15. Smith, S.J.; Burch, D.S. Relative Measurements of the Photodetachment for H^-. *Phys. Rev.* **1959**, *116*, 1125. [CrossRef]
16. Nahar, S.N. The Ultraviolet Properties of Evolved Stellar Population. In *New Quests in Stellar Astrophysics II*; Chavez, M., Bertone, E., Rosa-Gonzalez, D., Rodriguez-Merino, L.H., Eds.; Springer: New York, NY, USA, 2011; p. 245.
17. West, J.B.; Marr, G.V. The absolute photoionization of helium, neon, argon and krypton I the extreme vacuum ultraviolet region of the spectrum. *Proc. R. Soc. Lond. Ser. A Math. Phys. Sci.* **1976**, *349*, 397–421.
18. Samson, J.A.R.; He, Z.X.; Yin, L.; Haddad, G.N. Precision measurements of the absolute photoionization cross of He. *J. Phys. B* **1994**, *27*, 887. [CrossRef]
19. Madden, R.P.; Codling, K. New Autoionizing Atomic Energy Levels in He, Ne, and Ar. *Phys. Rev. Lett.* **1963**, *10*, 516–518. [CrossRef]
20. Bhatia, A.K.; Temkin, A. Calculation of autoionization of He and H^- using the projection-operator formalism. *Phys. Rev. A* **1975**, *11*, 2018–2024. [CrossRef]
21. Yan, M.; Sadeghpour, H.R.; Dalgarno, A. Photionization Cross Sections of He and H_2. *Astrophys. J.* **1998**, *496*, 1044. [CrossRef]
22. Norcross, D.W. Photoionization of the He metastable states. *J. Phys. B* **1971**, *4*, 652–657. [CrossRef]
23. Jacobs, V. Low-Energy Photoionization of the ^{11}S and ^{21}S states of He. *Phys. Rev. A* **1971**, *3*, 289–298. [CrossRef]
24. Daskhan, M.; Ghosh, A.S. Photoionization of He and Li^+. *Phys. Rev. A* **1984**, *29*, 2251–2254. [CrossRef]
25. Nahar, S.N. Photoionization and electron-ion recombination of He I. *New Astron.* **2010**, *15*, 417–426. [CrossRef]
26. Bhatia, A.K.; Drachman, R.J. Photoejection with excitation in H^- and other systems. *Phys. Rev. A* **2015**, *91*, 012702. [CrossRef]
27. Bhatia, A.K.; Temkin, A.; Silver, A. Photoionization of lithium. *Phys. Rev. A* **1975**, *12*, 2044–2051. [CrossRef]
28. Komninos, Y.; Nicolaides, C.A. Many-electron approach to atomic photoionization: Rydberg series of resonances and partial photoionization cross sections in helium, around the $n = 2$ threshold. *Phys. Rev. A* **1986**, *34*, 1995–2000. [CrossRef] [PubMed]
29. Jacobs, V.L.; Burke, P.G. Photoionization of He above the $n = 2$ threshold. *J. Phys. B* **1972**, *5*, L67. [CrossRef]
30. Dasgupta, A.; Bhatia, A.K. Photoionization of sodium atoms and electron scattering from ionized sodium. *Phys. Rev. A* **1985**, *31*, 759–771. [CrossRef]

31. Butler, K.; Mendoza, C. Accuracy of excitation and ionization cross sections. *J. Phys. B* **1983**, *16*, L707. [CrossRef]
32. Bhatia, A.K. Transitions (1s2p) $^3P^o$–(2p^2) $^3P^e$ in He and (2s2p) $^3P^o$–(2p^2) $^3P^e$ in H^-. *Phys. Rev. A* **1970**, *2*, 1667. [CrossRef]
33. Jacobs, V.L.; Bhatia, A.K.; Temkin, A. Photodetachment and Radiative Attachment involving the 2p^2 $^3P^e$ state of H^-. *Astrophys. J.* **1980**, *242*, 1278. [CrossRef]
34. Bhatia, A.K.; Drachman, R.J. New calculation of the properties of the positronium ion. *Phys. Rev. A* **1983**, *28*, 2523–2525. [CrossRef]
35. Bhatia, A.K.; Drachman, R.J. Photodetachment of the positronium negative ion. *Phys. Rev. A* **1985**, *32*, 3745–3747. [CrossRef] [PubMed]
36. Ward, S.J.; Humberston, J.W.; McDowell, M.R.C. Elastic scattering of electrons from positronium and photodetachment of positronium negative ion. *J. Phys. B* **1987**, *20*, 127. [CrossRef]
37. Bhatia, A.K. Photodetachment of the Positronium Negative Ion with Excitation in the Positronium Atom. *Atoms* **2019**, *7*, 2. [CrossRef]
38. Iallement, R.; Quemerais, E.; Bartex, J.-L.; Sandel, B.R.; Izamodenov, V. Voyager measurements of Hydrogen Lyman-α Diffuse Emission from the milky Way. *Science* **2011**, *334*, 1665–1669. [CrossRef] [PubMed]
39. Bhatia, A.K. *P*-wave electron-Be^{3+}, C^{5+}, and O^{7+} elastic scattering and photoabsorption in two-electron systems. *J. At. Mol. Condens. Nano Phys.* **2014**, *1*, 71–86. [CrossRef]
40. Tenorio, B.N.C.; Nascimento, M.A.C.; Coriani, S.; Rocha, A.B. Coupled Cluster Study of Photoionization and Photodetachment Cross Sections. *J. Chem. Theory Comput.* **2016**, *12*, 4440–4459. [CrossRef]
41. Andric, L.; Baccarelli, I.; Grozdanov, T.; McCarroll, R. Calculations of photodissociation cross sections by the smooth exterior complex scaling method. *Phys. Lett. A* **2002**, *298*, 41–48. [CrossRef]
42. Pegg, D.J. Interacting beam measurements of photodetachment. *Nucl. Instrum. Methods Phys. Res. B Beam Interact. Mater. Atoms* **1995**, *99*, 140. [CrossRef]
43. Ruberti, M.; Yun, R.; Gokhberg, K.; Kopelke, S.; Cederbaum, L.S.; Tarantelli, F.; Averbukh, V. Total photoionization cross-sections of excited electronic states by the algebraic diagrammatic construction-Stieltjes-Lanczos method. *J. Chem. Phys.* **2014**, *140*, 184107. [CrossRef] [PubMed]
44. Broad, J.T.; Reinhardt, W.P. Calculation of photoionization cross sections using L^2 basis sets. *J. Chem. Phys.* **1974**, *60*, 2182–2183. [CrossRef]
45. Joachain, C.J. *Quantum Scattering Theory*; North-Holland Publishing Company: New York, NY, USA, 1975; p. 654.
46. Nahar, S.N. Photoionization and Electron-Ion Recombination of n = 1 to Very High n-Values of Hydrogenic Ions. *Atoms* **2021**, *9*, 73. [CrossRef]
47. Paul, S.; Ho, Y.K. Hydrogen Atom in Debye Plasma. *Phys. Plasmas* **2009**, *16*, 06302. [CrossRef]
48. Kar, S.; Ho, Y.K. Photodetachment of the hydrogen negative ion in weakly coupled plasmas. *Phys. Plasmas* **2008**, *15*, 13301. [CrossRef]
49. Sahoo, S.; Ho, Y.K. Photoionization of Li and Na in Debye plasma environments. *Phys. Plasmas* **2006**, *13*, 63301. [CrossRef]
50. Chandrasekhar, S.; Breen, S. On the continuous absorption coefficient of the negative hydrogen ion. *Astrophys. J.* **1946**, *104*, 430. [CrossRef]
51. Gopalswamy, N. Positron Processes in the Sun. *Atoms* **2020**, *8*, 14. [CrossRef]
52. Lenard, P. Uber die lichtelektrische Wirkung. *Ann. Phys.* **1902**, *8*, 149. [CrossRef]